Asymmetrical effects in a 2D stenosis
MS N. BD288

P.-Y. Lagrée [1] *, A. Van Hirtum [2], X. Pelorson [2],
(1) Lab. de Modélisation en Mécanique, UMR CNRS 7607, B 162,
Université Paris 6, 75252 Paris France,
(2) Institut de la Communication parlée, I.N.P.G, Grenoble, France.

March 15, 2006

Abstract

An integral Interacting Boundary Layer theory is presented for the steady laminar flow in a asymmetrical bidimensional channel at high Reynolds number. The effect of asymmetry of the geometry is taken into account into the ideal fluid pressure expression. The effect is small but noticeable. Comparison with a Navier Stokes solution shows the trend of asymmetry: increasing the pressure drop on the more curved wall, decreasing it on the other. Separation and reattachment of the boundary layer are obtained and compare well.

1   Introduction

Computing the flow in locally constricted pipe is important in numerous applications in biomechanics. Of course this can be achieved with accuracy through Navier-Stokes solvers. For example, in local constrictions of blood vessels (Berger and Jou [1], Siegel et al. [20]), in veins (collapsible tubes Luo & Pedley [14]) in aneurysms (or dilated tube, Budwig et al. [2]), or in the upper airway (Shome et al. [19]). Here we will focus on steady laminar flows at high Reynolds number that can be considered as bidimensional, but not symmetrical. A typical example is on figure 1. In fact we will study a model example. Our aim is to present the simplest model for steady laminar pipe flow at large Reynolds number and to observe the effect of asymmetry.

We will compare some NS (Navier Stokes) solutions to solutions of asymptotic equations because we think that they provide a better understanding of the flow structure and relevant scalings. Using asymptotic equations, computational time is drastically reduced. Therefore, parameters may be changed easily and their influence can be thoroughly investigated.

---

*Corresponding author: e-mail: pyl@ccr.jussieu.fr, web: www.lmm.jussieu.fr/~lagree, Phone: +00 33 44272559, Fax: +00 33 44275259

Most of such simplified previous studies considered symmetrical flows (Pelorson et al. [16], Lorthois et al. [13], Lagrée et al. [10], Lagrée et al. [11], de Bruin et al. [6] and Kalse et al. [9]). In [10] and [9] it was observed that integral Interacting Boundary Layer and NS give very similar results. Predictive simplified formula for values of the skin friction and for the pressure drop based on the boundary layer were presented in [13] and [10]. In [11], the links between the "Triple Deck" theory and Interactive Boundary Layers in internal flows is presented. Furthermore [9] proposed part of the equations for a non symmetrical channel but did not solved them. Hence, we present an asymptotic derivation of the effect of non symmetry in the framework of the Interactive Boundary Layer theory (IBL). This theory is presented in Cebeci & Cousteix [3] or Sychev et al. [22], as not complete in the asymptotical framework. But, they point out that numerous results of calculations for different flows showed good agreement with experimental data in the description of flow separation in aerodynamics. In Veldman [24] the IBL and its links with the "Triple Deck" theory in open flows is explained. Some industrial examples comparing IBL and experiments are presented too.

Mainly, the descriptions of IBL use the length of the bump as fundamental scale (say L). The Reynolds number is then constructed with this length ($R_L = U_0 L / \nu$, here we are in a 2D channel, h_0 is the distance between the two plates, and $U_0 h_0$ is the flux). The boundary layer is then scaled by $L R_L^{-1/2}$, the displacement thickness is about $1.7 L R_L^{-1/2}$. This length L must be smaller that the length of entry (say L_e) which is such that the two boundary layers merge between the plates: $L_e R_{L_e}^{-1/2} = h_0$. This length is $L_e = h_0 (U_0 h_0 / \nu)$. The idea of the IBL theory is to couple the ideal fluid flowing in the core to variations of the displacement thickness of the boundary layer. For example, before the constriction, where the walls are flats, it means that the ideal fluid in the pipe experiments no more the section h_0 but a smaller section reduced by twice $1.7 L R_L^{-1/2}$. So the flow is accelerated. In "classical boundary layer theory" it is impossible: the Reynolds is infinite ($R_L^{-1/2} = 0$). The entry length is reject at infinity. This boundary layer effect is an order two effect (Van Dyke [23]), the velocity remains U_0. But in "IBL theory" this is possible. It means that $R_L^{-1/2}$ is small but not so much. Hence, effect of second order and first order are mixed: the boundary layer retroacts on the ideal fluid. This was the paradox of IBL.

But, recently, Dechaume et al. [7] (and Cousteix and Mauss [4] and [5]) established on rational basis the IBL equations. They break the paradox. They use a "modified Van-Dyke" principle and "successive complementary expansion method". The existence of a small parameter in the equation is then no more a problem. The link with "Triple Deck" theory is done as well. They show that with this technique the IBL equations are fully justified.

Here, as we are in pipe, we prefer to use h_0 to construct the Reynolds

($Re = U_0 h_0 / \nu$) and to scale the boundary layer. So to have a small boundary layer as just mentioned, we have to be near the entrance of the pipe at a distance smaller than $L_e = h_0 (U_0 h_0 / \nu)$ (so that we are before the merging of the boundary layers). Compared to the previous approach where we gave L, it is just a change of scale of the boundary layer equations. This length must be larger than the distance between the plates in order to do the expansion in the ideal fluid. But we will observe that the system is very robust and may be used even if the width of the bump is h_0. One reason of this robustness is that the flow is accelerated, so that the boundary layer is thinner. The other one belongs to magic of asymptotic expansion which give often good results even if the small parameter is not so small (Van Dyke [23]).

First we present the problem and the basic scales for the NS problem. Then we introduce a simplified set of equations: Reduced Navier Stokes. The integral IBL system is introduced thereafter. A comparison between the three models shows that the integral IBL catches most of flow features (with a very short computational time, about 500 times less).

2 Equations

2.1 Navier Stokes

We solve the Newtonian steady laminar incompressible bidimensional Navier Stokes equations with the numerical code Castem 2000 [15]. The geometry consists in a straight channel with a bump on one wall (figure 1), we used the channel height h_0 to nondimensionalise the scales of x^* and y^*. A Poiseuille velocity (of total flux $U_0 h_0$ equal to 1 in non dimensional scales) is imposed at the entrance, a zero stress is imposed at exit. The exit and the entrance are far enough from the stenosis to avoid their influences. We present (on fig. 1 to 5) only results for $Re = 500$ ($Re = U_0 h_0 / \nu$). Increasing the Reynolds increases the number of points and the computational time. It creates problems at the output where the jet may oscillate. But we do not focus here on the NS problem.

2.2 Reduced Navier Stokes

We now present two simplifications of the NS equations issued from boundary layer theory (Schlichting [18], Sychev et al. [22], Rubin and Tannehill [17]). The first simplification consists in neglecting the transverse variation of pressure. This leads to a system we call RNSP (Reduced Navier Stokes/ Prandtl) because this is a reduced system obtained from Navier Stokes and because this is in fact the Prandtl partial differential equations (with different boundary condition than in the classical boundary layer theory). It has been shown that this system is a good approximation of NS in symmetrical stenoses (Lagrée et al. [10]) and that its axisymmetrical version (Lagrée &

Lorthois [11]) includes most of IBL/ Triple Deck/ Double Deck asymptotical régimes. These equations are obtained from NS by supposing that the transverse scale is smaller than the longitudinal one and that the Reynolds number is large. To settle the equations, u^* is scaled by U_0, v^* by U_0/Re, x^* by $h_0 Re$, y^* by h_0 and p^* by ρU_0^2. The flow is supposed quasistatic: Strouhal number is low, in fact the spatial acceleration is large. The system is:

$$\frac{\partial}{\partial x}u + \frac{\partial}{\partial y}v = 0, \qquad u\frac{\partial}{\partial x}u + v\frac{\partial}{\partial y}u = -\frac{\partial}{\partial x}p + \frac{\partial^2}{\partial y^2}u, \qquad 0 = -\frac{\partial}{\partial y}p. \quad (1)$$

The boundary conditions are no slip $u(x, y = f_b(x)) = 0$, $v(x, y = f_b(x)) = 0$ at the lower wall defined by $f_b(x)$ (whose dimension is h_0) and at the upper wall $u(x, y = 1 - f_h(x)) = v(x, y = 1 - f_h(x)) = 0$. At the entrance, pressure is zero, the first velocity profile is given (for example a flat profile $u = 1$, $v = 0$, or Poiseuille).

We note the invariance by Prandtl transform ($y^p = y - f_b(x)$) that allows to solve the problem from $y^p = 0$ to $y^p = 1 - f_h(x) - f_b(x)$.

We note that there are two transverse boundary conditions ($u(x, y = f_b(x)) = 0$ and $u(x, y = 1 - f_h(x))$) but there is no outflow boundary condition (only $u = 1$ is given at the entrance). This is because the system is parabolic in x ($u\partial_x u \simeq \partial_y^2 u$). The Navier Stokes equations must have an output condition, which is not the case here.

2.3   IBL

2.3.1   Ideal Fluid

Previous studies used mainly a symmetrical approximation, so that ideal fluid pressure or ideal fluid velocity was a function of the longitudinal variable alone. We want to introduce a small effect of transverse variation of pressure. Then we will couple the ideal fluid with the two boundary layers.

We solve linearized Euler equations in a channel with a slowly varying indentation with ($\xi = \varepsilon x^*/h_0$, $y = y^*/h_0$). Thereafter ξ will be identified with x. In practice, we will discuss the flow with a flat upper wall ($y_h = 1$ or $f_h = 0$), with an indentation at the lower wall ($y_b = f_b$). The maximum value of f_b is α the degree of stenosis, the indentation may be severe, it means that α may be close to 1. Expanding as:

$$u = U_0(\xi) + \varepsilon u_1(\xi, y) + \varepsilon^2 u_2(\xi, y) + ..., \tag{2}$$

$$v = \varepsilon v_1(\xi, y) + \varepsilon^3 v_3(\xi, y) + ..., \tag{3}$$

$$p = p_0(\xi) + \varepsilon p_1(\xi, y) + \varepsilon^2 p_2(\xi, y) + ..., \tag{4}$$

so that Euler system (we note that the perturbations u_1 and p_1 are zero) is at order 0 and 1:

$$U_0 \frac{\partial U_0}{\partial \xi} = -\frac{\partial p_0}{\partial \xi}, \tag{5}$$

4

and

$$\varepsilon \frac{\partial U_0}{\partial \xi} + \varepsilon \frac{\partial v_1}{\partial y} = 0. \tag{6}$$

(The flow was supposed irrotational $\partial_y U_0 - O(\varepsilon^2) = 0$). Writing the no slip condition on the upper and lower walls (resp. y_h and y_b):

$$v_1(\xi, y_b = f_h) = U_0 \frac{\partial f_b}{\partial \xi}, \qquad v_1(\xi, y_h = 1 - f_h) = -U_0 \frac{\partial f_h}{\partial \xi},$$

we integrate twice the continuity equation (6) to obtain the classical expression of U_0 and by the momentum equation (5) we obtain P_0:

$$U_0(\xi) = \frac{1}{1 - f_b(\xi) - f_h(\xi)}, \qquad P_0(x) = \frac{1}{2} - \frac{1}{2}\Big(\frac{1}{1 - f_b(\xi) - f_h(\xi)}\Big)^2. \tag{7}$$

The expression for transverse velocity follows:

$$v_1(\xi, y) = U_0 \frac{\partial f_b}{\partial \xi} + \frac{y - f_b}{1 - f_h - f_b}\Big(-U_0 \frac{\partial f_b}{\partial \xi} - U_0 \frac{\partial f_h}{\partial \xi}\Big) \tag{8}$$

The next order is:

$$\varepsilon^2 U_0 \frac{\partial v_1}{\partial \xi} = -\varepsilon^2 \frac{\partial p_2}{\partial y}, \tag{9}$$

$$\varepsilon^3 \frac{\partial U_0 u_2}{\partial \xi} = -\varepsilon^3 \frac{\partial p_2}{\partial \xi}, \tag{10}$$

$$\varepsilon^3 \frac{\partial u_2}{\partial \xi} + \varepsilon^3 \frac{\partial v_3}{\partial y} = 0. \tag{11}$$

From the integration by y of the incompressibility at order 0 and 2, we obtain that $\partial_\xi(\int_{y_b}^{y_h}(U_0 + \varepsilon^2 u_2)dy) = 0$, once developed using (8) and from Euler equation (10) we then obtain $\int_{y_b}^{y_h} p_2 dy = 0$. After some algebra, from (9) and (8), we find the pressure value at order 2 on the lower wall:

$$p_2(\xi, f_b) = \frac{-4 f_b'(\xi)^2 - 2 f_b'(\xi) f_h'(\xi) + 2 f_h'(\xi)^2}{6 (-1 + f_b(\xi) + f_h(\xi))} +$$
$$+ \frac{(-1 + f_b(\xi) + f_h(\xi)) (2 f_b''(\xi) - f_h''(\xi))}{6 (-1 + f_b(\xi) + f_h(\xi))}, \tag{12}$$

and the pressure value at order 2 at the upper wall:

$$p_2(\xi, 1 - f_h) = \frac{-\Big(-2 f_b'(\xi)^2 + 2 f_b'(\xi) f_h'(\xi) + 4 f_h'(\xi)^2\Big)}{6 (-1 + f_b(\xi) + f_h(\xi))} +$$
$$+ \frac{(-1 + f_b(\xi) + f_h(\xi)) (f_b''(\xi) - 2 f_h''(\xi))}{6 (-1 + f_b(\xi) + f_h(\xi))}. \tag{13}$$

We define the total transverse pressure drop as $\varepsilon^2(p_2(\xi, y_h) - p_2(\xi, y_b))$, which is a bit more simple:

$$\varepsilon^2(p_2(\xi, y_h) - p_2(\xi, y_b)) = \varepsilon^2\Big(\frac{(f_h'(\xi)^2 - f_b'(\xi)^2)}{1 - f_b(\xi) - f_h(\xi)} + \frac{(f_h''(\xi) - f_b''(\xi))}{2}\Big). \quad (14)$$

Of course, a symmetrical channel ($f_b = f_h$) gives $\Delta P_0 = 0$, in practice we will use $f_h = 0$. We note that Kalse *et al.* [9] derived with more severe approximations this same pressure drop (but not (12) nor (13)). Here the result comes only from the hypothesis.

2.3.2 Boundary layer

Up to now in this section, we supposed that the fluid was ideal. Here we introduce the Boundary Layer equations which may be deduced from Navier Stokes supposing that the Reynolds number is large and that viscous effects are restricted to two thin layers near the walls (see figure 2). We simplify much more the boundary layer in using the integral Kármán equation ([18], [8]). We define δ_1^b and δ_1^h the displacement thicknesses at the lower and the upper walls. The choice of the scalling comes here from the RNSP case, x is scaled by $h_0 Re$ and $\delta_1^{b,h}$ by h_0, in fact the boundary layer will be small at those scales (see Lagrée & Lorthois [11]). This slow variation in x allows to identify Re^{-1} and ε. So, this gives the following system where the ideal fluid (computed in the preceding section) promotes the boundary layer. We have two boundary layers, one at the top:

$$\frac{d}{dx}\Big(\frac{\delta_1^h}{H}\Big) + \frac{\delta_1^h}{u_e^h}\Big(1 + \frac{2}{H}\Big)\frac{du_e^h}{dx} = \frac{f_2 H}{\delta_1^h u_e^h}, \qquad \delta_1^h = F(u_e^h), \qquad (15)$$

and another at the bottom:

$$\frac{d}{dx}\Big(\frac{\delta_1^b}{H}\Big) + \frac{\delta_1^b}{u_e^b}\Big(1 + \frac{2}{H}\Big)\frac{du_e^b}{dx} = \frac{f_2 H}{\delta_1^b u_e^b}, \qquad \delta_1^b = F(u_e^b). \qquad (16)$$

Initial condition is for example $\delta_1^{h,b}(0) = 0$ and $u_e^{h,b}(0) = 1$. In the classical approach, δ_1 is obtained through the knowledge of u_e, which we write formaly $\delta_1^{b,h} = F(u_e^{b,h})$. To solve these boundary layer equations, a closure relationship linking H and f_2 to the velocity and the displacement thickness is needed. This is of course a strong hypothesis. Defining $\Lambda_1 = \delta_1^2 \frac{du_e}{dx}$, (of course it is δ_1^b, u_e^b or δ_1^h, u_e^h) the system is closed from the resolution of the Falkner Skan system as follows:

$$H = \left\{ \begin{array}{ll} 2.5905e^{-0.37098\Lambda_1} & \text{if } \Lambda_1 < 0.6 \\ 2.074 & \text{if } \Lambda_1 > 0.6 \end{array} \right\}, \qquad f_2 = 1.05(-H^{-1} + 4H^{-2}).$$

It means that we suppose that each profile remains a Falkner Skan one in the boundary layer.

This closure allows flow separation for decelerated flows, we will see in the next section that one has to solve these equations (15 and 16) in an "inverse way" ($u_e^{b,h} = F^{-1}(\delta_1^{b,h})$) to compute flow separation.

Those simplifications are in the spirit of Lorthois *et al.* [13], but here in 2D. Recently, Kalse *et al.* [9] used nearly the same modelisation.

2.3.3 Integral IBL

The Integral Boundary Layer equations (IBL) suppose that the wall is no more at the bottom $y_b = f_b$ and at the channel height $y_h = 1 - f_h$ but it is changed by the amount of the displacement boundary layer thickness δ_1^h at the upper wall and δ_1^b at the lower wall. That is why we scaled $\delta_1^{b,h}$ by h_0 and why we identified ε to be Re^{-1} and $x = \xi$.

This gives a coupled system where the ideal fluid promotes the boundary layer: (15) and (16) that, in growing, retroacts (with the help of the concept of displacement thickness) on the ideal fluid through the flux conservation. The mean velocity (7) is no more $(1 - f_b(x) - f_h(x))^{-1}$ but is now $(1 - (f_b(x) + \delta_1^b(x)) - (f_h(x) + \delta_1^h(x)))^{-1}$. The ideal fluid relation is now:

$$P_0(x) = \frac{1}{2} - \frac{1}{2}\Big(\frac{1}{1 - (f_b(x) + \delta_1^b(x)) - (f_h(x) + \delta_1^h(x))}\Big)^2. \qquad (17)$$

Using IBL idea (where first and second order are mixed), we say that the pressure are in fact $p^b = P_0(x) + \varepsilon^2 p_b(x, y_b = 1 - (f_b + \delta_1^b))$ and $p^h = P_0(x) + \varepsilon^2 p_h(x, y_h = f_h + \delta_1^h)$. The pressure at the bottom $(p^b(x, y_b = f_b + \delta_1^b))$ is (12) with f_b changed by $f_b + \delta_1^b$; the same for $p^h(x, y_h = 1 - (f_h + \delta_1^h))$ which is (13) with f_h changed by $f_h + \delta_1^h$. As the expressions for $p^b(x, y_b = f_h + \delta_1^h)$ and $p^h(x, y_h = f_h + \delta_1^h)$ are a bit complicated, we just write their difference $p^h - p^b = \Delta P_0$:

$$\Delta P_0 = \varepsilon^2 \Big(\frac{((f_h' + \delta_1'^h)^2 - (f_b' + \delta_1'^b)^2)}{1 - (f_b + \delta_1^b) - (f_h + \delta_1^h)} + \frac{\left(f_h'' + \delta_1''^h - f_b'' - \delta_1''^b\right)}{2}\Big). \qquad (18)$$

Note that we recover a result that looks like Smith [21] result in pipe flow, the transversal perturbation of pressure in a perturbed Poiseuille flow is $p_h - p_b = A''/30$ where $-A$ is a displacement of the stream lines as $\delta_1^b - \delta_1^h$ is. Of course the two configurations are very different.

We note that this coupling relation produces upstream influence, it means that before the bump, the flow "knows" that it is comming. This creates solutions in e^{kx} with $k > 0$, we see it on the numerical solutions.

2.3.4 Numerical resolution of the Integral IBL

We solve the interactive system by a semi inverse method (Le Balleur [12]). This means that the boundary layer is solved in an inverse way (the displacement thickness is imposed and the velocity is a result of the computation).

This inverse way allows to compute flow separation (the direct way would lead to a singularity at separation). The ideal fluid is computed in "direct way" from the geometry changed by the amount of the boundary layer displacement thickness.

At iteration n, we have a set of two displacement boundary layer thickness $(\delta_1^b)^n$ and $(\delta_1^h)^n$. They give, by solving in an inverse way (15) and (16), two associated boundary layer velocities: $(u_e^h)^n = F^{-1}((\delta_1^h)^n)$ and $(u_e^b)^n = F^{-1}((\delta_1^b)^n)$.

The two corresponding pressures in the boundary layers $(p_e^h)^n$ and $(p_e^b)^n$ are computed from these velocities, i.e. Bernoulli:

$$(p_e^{(b,h)})^n = \frac{1}{2}(1 - ((u_e^{(b,h)})^n)^2). \tag{19}$$

From the expressions of $p^h(x, y_h = f_b + \delta_1^b))$ and $p_b(x, y_b = f_b + \delta_1^b))$ (defined before equation 18), the ideal fluid pressures are computed. A new boundary condition associated to the second derivative must be used. At the output $\frac{\partial p^h}{\partial x} = 0$ and $\frac{\partial p^b}{\partial x} = 0$ are imposed.

The semi inverse relaxation is done as follows (figure 3):

$$(\delta_1^h)^{n+1} = (\delta_1^h)^n + \lambda((p^h)^n - (p_e^h)^n) \tag{20}$$
$$(\delta_1^b)^{n+1} = (\delta_1^b)^n + \lambda((p^b)^n - (p_e^b)^n). \tag{21}$$

The relaxation parameter λ is chosen by trial and error in order to obtain convergence. In order to obtain estimate of λ the theory proposed by Le Balleur [12] is relevant.

3 Some numerical comparisons

We compare then the NS results to the RNSP and IBL results. We suppose that the upper wall is flat $f_h = 0$, and that the lower wall is a given function of x^*, for example the following function is close to half a circle:

$$\zeta = \frac{x^* - x_c^*}{4\alpha h_0/3}, \qquad f_b(\zeta) = 1 - \frac{\zeta^2}{2} - \frac{\zeta^4}{8} - \frac{\zeta^6}{16} + \frac{1445\zeta^8}{13122} - \frac{1385\zeta^{10}}{59049},$$

which is nearly $\sqrt{1 - \zeta^2}$ around $\zeta = 0$ up to order ζ^8. Notice that on every figure we used the physical longitudinal scale (h_0) to plot the curves; numerically in (1) and (15, 16), the width of the bump is of order $(1/Re)$ in our scales.

The first curves show the pressure (Fig. 4) and the skin friction (Fig 5) computed by RNSP and NS. We see that the pressure $p(x)$ from RNSP is an approximation of the mean NS pressure. The NS pressure displays a larger drop just after the throat on the curved wall and a smaller pressure

drop on the flat wall. The recompression is over predicted by RNSP. In the symmetrical cases ([11]) the difference was smaller.

The RNSP skin friction overall distribution looks like the NS one. There is a kink in the skin friction at the flat wall which does not exist in NS because of the smoother pressure gradient on the flat wall.

The next curves show the pressure (Fig. 6) and the skin friction (Fig. 7) computed by integral IBL and NS. They show "upstream influence", the upstream part of the flow is influenced by the downstream part. On the pressure curve, before the throat, the upstream influence of the bump is to produce an over pressure drop on the curved wall. This upstream influence comes from the order two derivative in the transverse pressure relation (Eq 18), it has an exponential behavior (e^{kx} with $k > 0$). This influence is responsible for the incipient separation before the bump, increasing α leads to flow separation before the bump. This upstream influence is due to the curvature of the stream line. It does not exist in the symmetrical case.

The integral IBL skin friction looks like the NS one, but it is overestimated by the IBL (results from integral IBL will never be perfect because there is a strong closure hypothesis). The integral IBL well predicts the position of the point of separation but overpredicts the negative skin friction. The incipient separation before the bump is well predicted and is related to the upstream influence.

The displacement functions δ_1^b and δ_1^h (IBL flat) are plotted on figure (Fig. 8). A large value of the displacement thickness is associated to a deceleration of the flow and eventually to boundary layer separation. A thin value is associated to the large acceleration at the throat. The difference of pressure $p^h - p^b$ is plotted too. As this difference of pressure has scale Re^{-2} the effect of asymmetry becomes smaller with larger Re.

The integral IBL gives good trends in the influence of asymmetry, its main advantage is that it is a extremely quick method compared to full Navier Stokes which is time and memory consuming. For example, using a Linux x86 workstation at 3.0 GHz we may roughly compare the three methods. Navier Stokes solver CASTEM takes about 15 minutes to compute the flow (200 times 16 nodes) for a maximal error of 10^{-5} between two iterations. RNSP solver takes 2 seconds to compute the flow (on a very fine mesh 3000 times 1000). Finally, the integral IBL solves a symmetrical case in less than 0.5 second; it needs 2 more seconds to obtain a maximal error of 10^{-5} between two iterations in the non symmetrical case (in about 800 iterations). Those figure are indicative, faster NS solvers may exist, and our code is not optimised.

Increasing the Reynolds number will disadvantage the Navier Stokes computation: the IBL remains always precise, but the NS mesh has to be refined.

4 Conclusion

We have presented here a simplified model issued from asymptotic analysis. The expressions of the pressure at the upper and lower wall were presented. The effect of asymmetry is an order two effect. The integral Boundary Layer equations are solved together with the ideal fluid equations thanks to Interactive Boundary Layer Theory.

A symmetrical pipe has no upstream influence, it means that changing the downstream conditions does not change the flow upstream. This is broken by the asymmetry. Concerning the pressure, the effect of asymmetry is to increase the pressure drop at the curved bottom wall and to lower the pressure at the flat upper wall. The smallest pressure is on the curved wall, the minimum pressure on the bottom wall is more upstream that the pressure minimum on the top wall. The two minima are after the throat. A massive separation appears after the throat on the curved wall, a small separation appears before the throat on the curved wall, no separation occurs at the flat wall. The effect of downstream on upstream that is not present in the RNSP theory is a pure effect of the wall and displacement curvature. This effect creates an increase of pressure on the lower wall which is responsible for the upstream flow separation.

Solving the equations of IBL theory is very fast (from factor 2000 in the symmetrical case to a factor 500 in the non-symmetrical case), so we plan to use it in biomecanical fluid structure interactions such like the Obstructive Sleep Apnea syndrome.

References

[1] Berger S. A. and Jou L-D. (2000): "Flows in stenotic vessels", Annu. Rev. Fluid Mech. 2000. 32, pp. 347-382.

[2] Budwig R., Elger D., Hooper H. & Slippy J. (1998): "Steady flow in abdominal aortic aneurysm models", J. Biomech. Eng., vol 115, nov., pp. 419- 423.

[3] Cebeci T. & Cousteix J. (1999): "Modeling and computation of boundary layer flows", Springer Verlag.

[4] Cousteix J., & Mauss J. (2004): "Approximations of the Navier-Stokes equations for high Reynolds number flows past a solid wall" Journal of Computational and Applied Mathematics 166(1): 101-122, 2004.

[5] Cousteix J., & Mauss J. (2006): "Analyse asymptotique et couche limite", Mathématiques et Applications, Vol. 56 2006, XII, 396 p.

[6] de Bruin B., Lagrée P.-Y., Lorthois S., Vilain C., Veldman A.E.P. (2001): "Comparison of Navier Stokes and Reduced Navier Stokes unsteady computation in a stenosis", Archives of Physiology and Biochemistry Vol 109 sept 2001, p 79.

[7] A. Dechaume, J. Cousteix and J. Mauss (2005): "An interactive boundary layer model compared to the triple deck theory", European Journal of Mechanics - B/Fluids, Volume 24, Issue 4, July-August, pp. 439-447.

[8] Gersten, K. and Hervig, H. (1992): "Strömungsmechanik : Grundlagen der Impuls-Wärme-und Stoffübertragung aus asymptotischer Sicht", Vieweg, Wiesbaden.

[9] Kalse S. G. C., Bijl H., and van Oudheusden B. W. (2003): "One-Dimensional Viscous-Inviscid Strong Interaction Model for Flow in Indented Channels With Separation and Reattachment", Journal of Biomechanical Engineering, Volume 125, Issue 3, pp. 355-362.

[10] Lagrée P.-Y., Berger E., Deverge M., Vilain C. & Hirschberg A. (2005): "Characterization of the pressure drop in a 2D symmetrical pipe: some asymptotical, numerical and experimental comparisons", ZAMM, vol 85, No 2, pp. 141-146.

[11] P.-Y. Lagrée & S. Lorthois (2005): "The RNS/Prandtl equations and their link with other asymptotic descriptions. Application to the computation of the maximum value of the Wall Shear Stress in a pipe", Int. J. Eng Sci., Vol 43/3-4 pp 352-378.

[12] La Balleur J.C., (1978): "Couplage visqueux non-visqueux: méthode numérique et applications aux écoulement bidimensionnels transsoniques et supersoniques", la recherche Aérospatiale, 2, pp. 67-76, Eng Trans ESA TT-496.

[13] S. Lorthois, P.-Y. Lagrée, J.-P. Marc-Vergnes & F. Cassot. (2000): "Maximal wall shear stress in arterial stenoses: Application to the internal carotid arteries", Journal of Biomechanical Egineering, Volume 122, Issue 6, pp. 661-666.

[14] Luo X. Y. & Pedley T. J., (1998): "The effects of the wall inertia on the 2-D collapsible channel flow", J of Fluid Mechanics, Vol. 363, pp. 253-280.

[15] H. Paillère et F. Dabbene: Initiation à la simulation numérique en mécanique des fluides à l'aide de Castem 2000, éditions ENSTA .

[16] Pelorson X., Hirschberg A., van Hassel R.R. , Wijnands, A.P.J., Auregan Y., (1994): "Theoretical and experimental study of quasisteady

flow separation within the glottis during phonation", J. Acoust. Soc. Am 96, p. 3416-3431.

[17] S G Rubin, J C Tannehill (1992): "Parabolized/Reduced Navier-Stokes Computational Techniques", Annual Review of Fluid Mechanics, January 1992, Vol. 24, Pages 117-144

[18] H. Schlichting (1987): "Boundary layer theory" , 7th ed Mc Graw Hill.

[19] B. Shome, L. Wang, M. Santare, A. Prasad, A. Szeri, & D. Roberts (1998): "Modeling of Airflow in the Pharynx With Application to Sleep Apnea", vol 120, 3, pp. 416- 422.

[20] Siegel J.M, Markou C.P., Ku D.N., & Hanson, S.R (1994): "A scaling law for wall shear stress through an arterial stenosis", ASME J. Biomeh. Eng. 116, 446- 451.

[21] F. T. Smith (1976): "Flow through constricted or dilated pipes and channels", part 1 and 2, Q. J. MEch. Appl. Math. vol 29, pp 343- 364 & 365- 376.

[22] V. V. Sychev, A. I. Ruban, Vic. V. Sychev, G. L. Korolev (1998): 'Asymptotic Theory of Separated Flows. Cambridge University Press', 378p.

[23] Van Dyke M. (1975): "Perturbation Methods in Fluid Mechanics" Parabolic Press.

[24] A.E.P. Veldman (2001): "Matched asymptotic expansions and the numerical treatment of viscous-inviscid interaction", Journal of Engineering Mathematics, Volume 39, Issue 1, March, pp. 189 - 206

/Users/pyl/Desktop/bureau/mi_co/APNEEE/TEX/anesym.tex
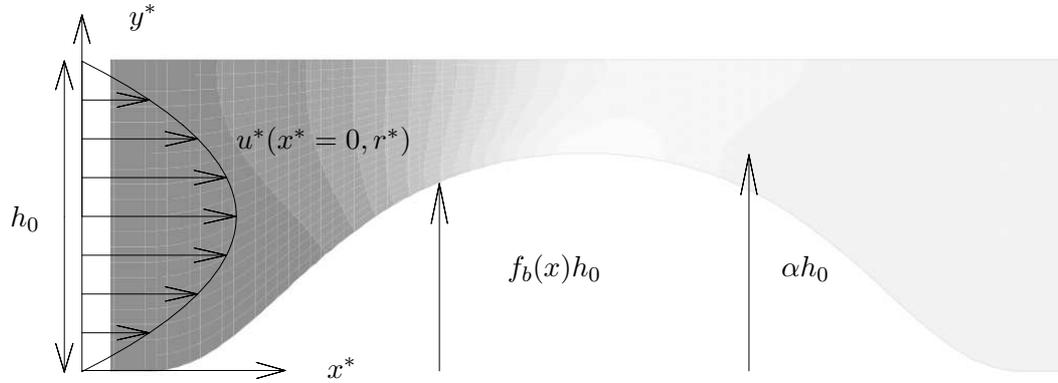
Figure 1: A zoom of the channel with its stenose. The constriction is a smoothed ellipsis (the lower wall is f_b, the upper is here flat, $f_h = 0$). The transverse scale is adimensionalised by the unperturbed channel width h_0. Here, the entry profile is a Poiseuille profile ($u = U_{Pois} = y(1 - y)$ and $v = 0$), but any other is possible. The NS computational domain is larger to avoid entrance and output effects, iso pressure (gray scale) and the mesh (white grid) are plotted.
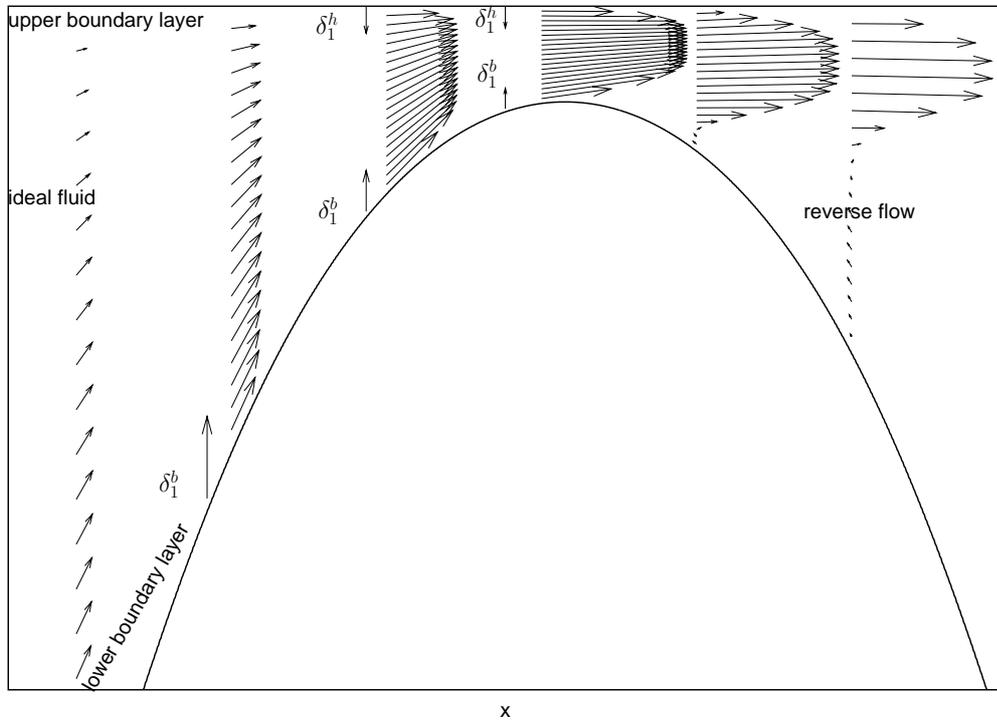
Figure 2: A larger zoom of the channel (here a RNSP computation at $Re = 500$) with the stenose and the upper flat wall. The two upper and lower boundary layers and the ideal fluid appear from the computation. The interaction between the ideal fluid and the boundary layers is the core of the Interactive Boundary Layer theory.
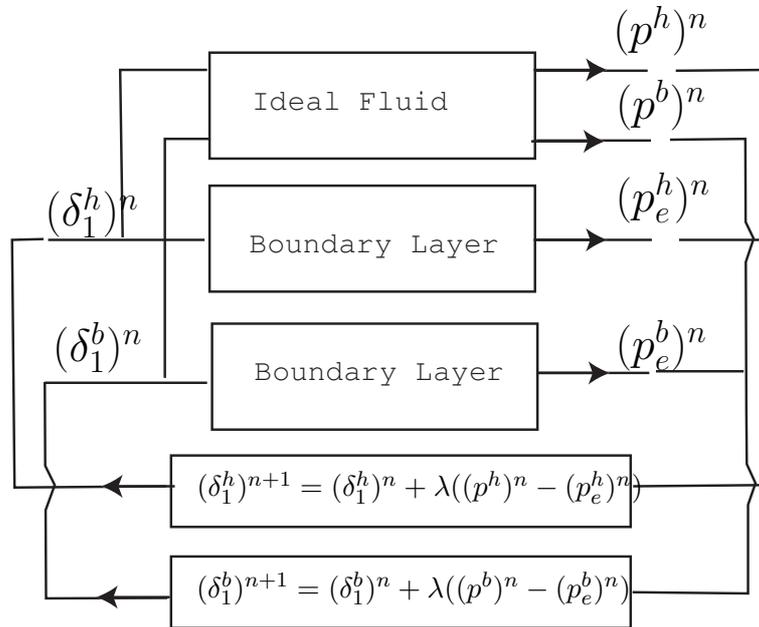
Figure 3: A chart of the iterative "semi inverse" interaction: the two boundary layers are solved in an inverse way. The correction of boundary layer thickness is proportional to the difference of pressure.
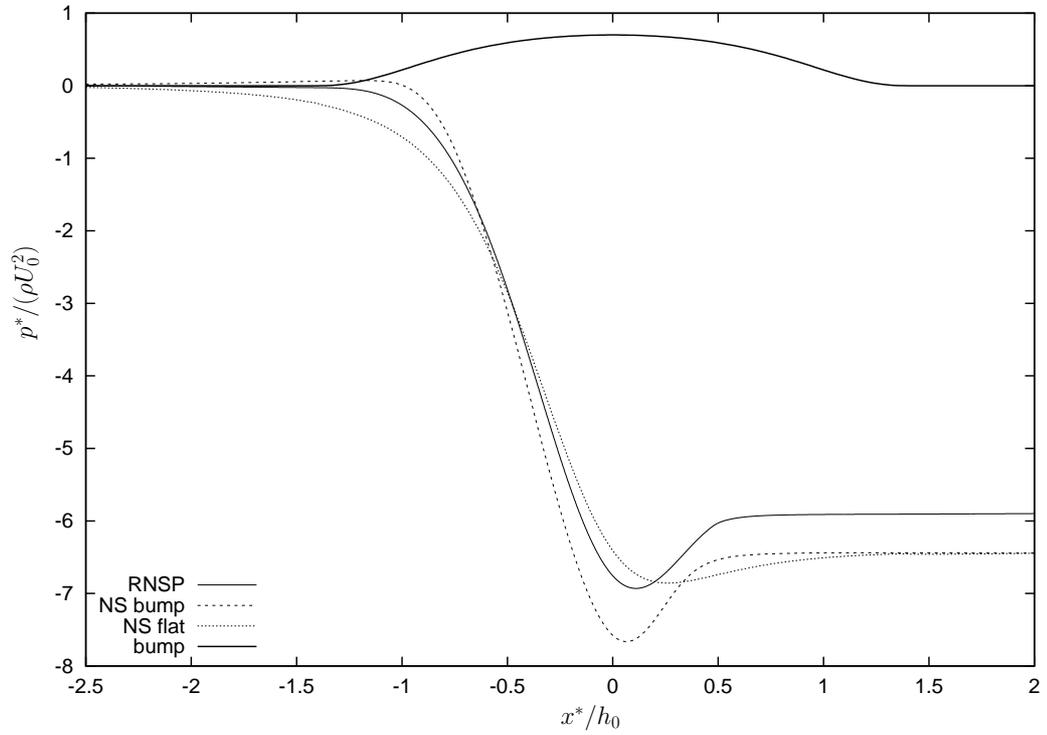
Figure 4: Comparison of RNSP and NS pressures, RNSP solution is an approximation of the two NS pressures. The geometry is plotted as well.
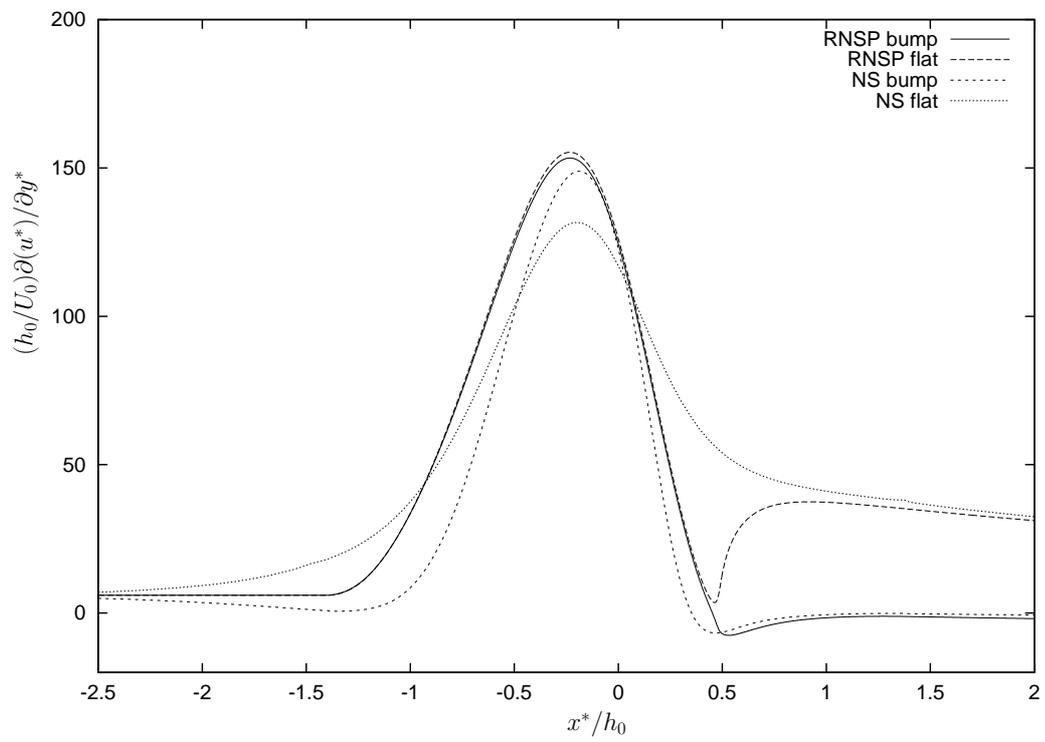
Figure 5: Comparison of RNSP and NS wall shear stress. The flat wall shear stress is over predicted by RNSP at the maximum, but in the wake $(x^*/h_0 > 1)$ it is better.

17
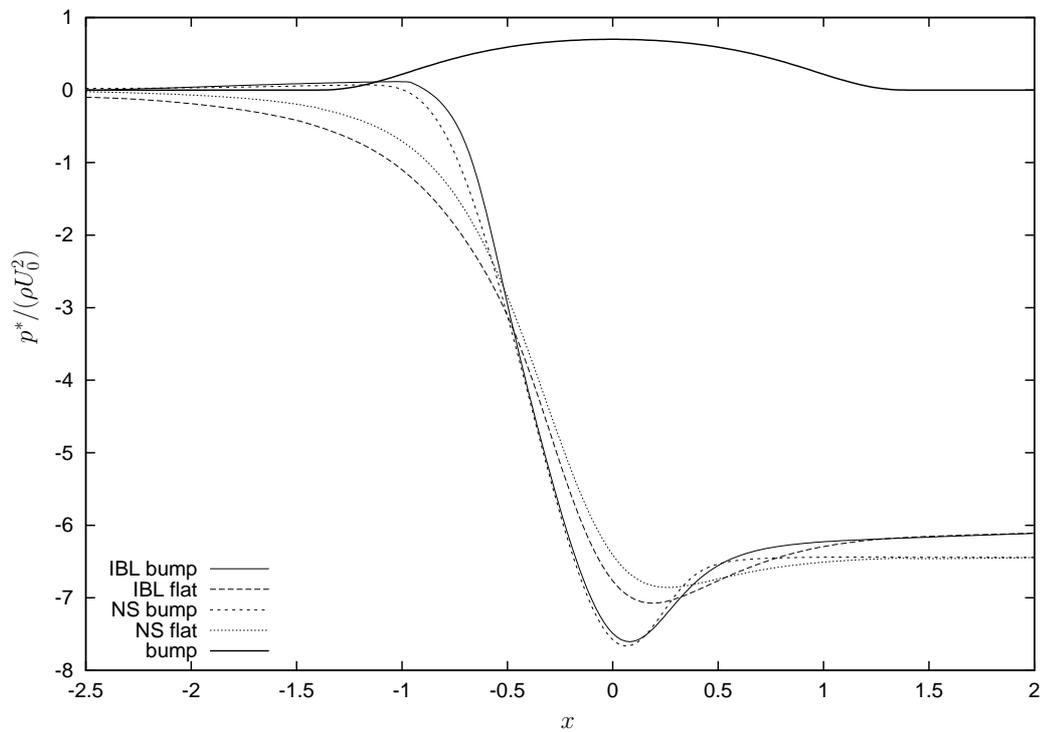
Figure 6: Comparison of integral IBL and NS pressures. The IBL approach well predicts the over pressure on the flat wall and the positions of the minima of of the pressures after the throat.
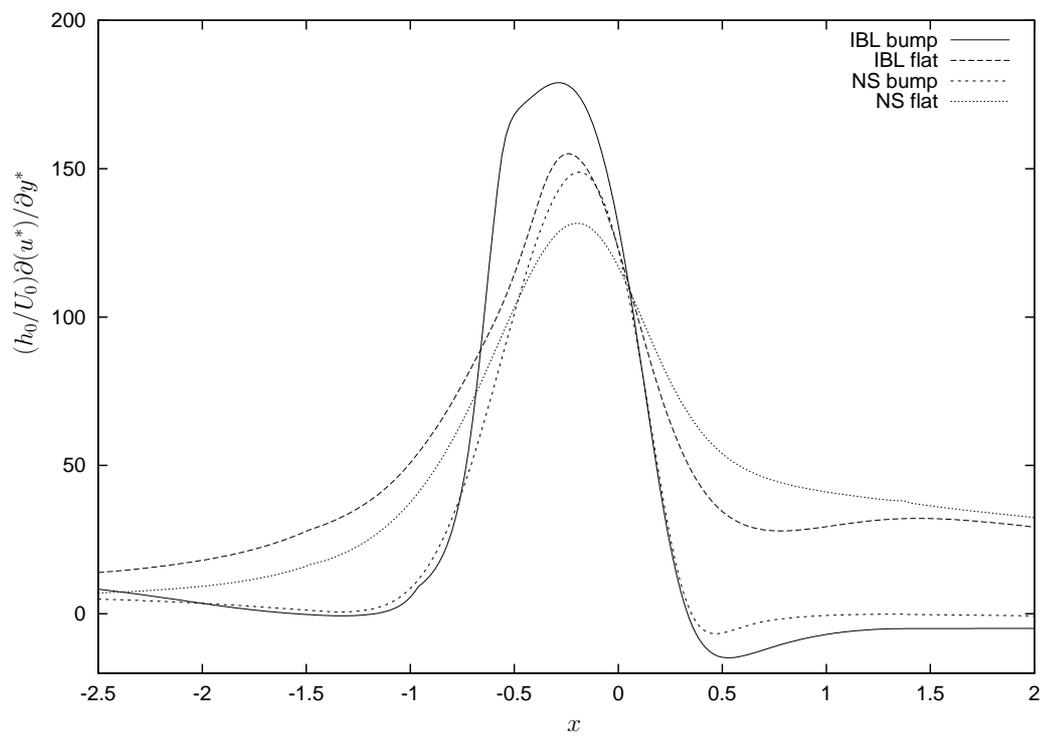
Figure 7: Skin friction, comparison of integral IBL and NS. The integral IBL over predicts the maximum of skin friction but well predicts the position of the point of separation. The incipient separation before the bump is well predicted.

19
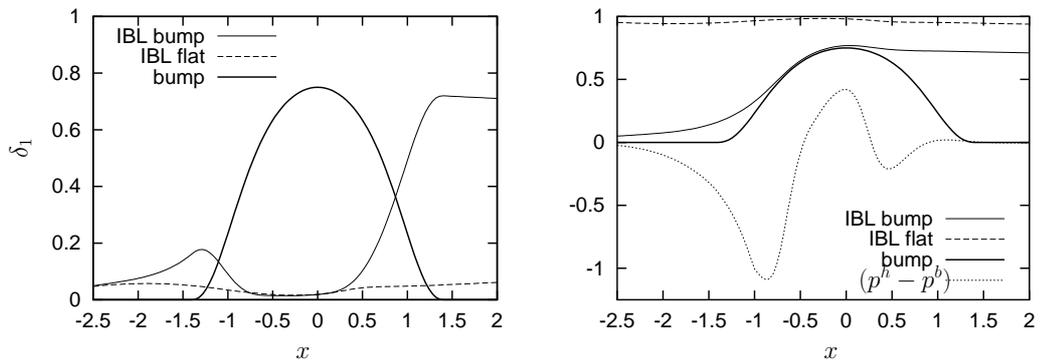
Figure 8: Left: the displacement functions δ_1^b (IBL bump) and δ_1^h (IBL flat). A large value of δ_1 is associated to boundary layer separation. A thin value is associated to the large acceleration at the throat. Right: the difference of pressure $p^h - p^b$ is plotted, the "final effective" channel is plotted: $1 - \delta_1^h$ and $f_b + \delta_1^b$; the jet due to separation is visible.